Silk I Structure Formation Through Silk Fibroin Self-Assembly

Jinfa Ming,[1] Baoqi Zuo[1,2]

[1]*College of Textile and Clothing Engineering, Soochow University, Suzhou 215021, China*
[2]*National Engineering Laboratory for Modern Silk, Soochow University, Suzhou 215123, China*

Received 27 July 2011; accepted 8 October 2011
DOI 10.1002/app.36354
Published online 20 January 2012 in Wiley Online Library (wileyonlinelibrary.com).

ABSTRACT: Regenerated silk fibroin films are normally produced by increasing the Silk II structure (β-sheet content). In the present study, silk fibroin films were prepared by controlling the environmental temperature and humidity, resulting in the formation of silk films with a predominant Silk I structure instead of Silk II structure. Wide angle X-ray diffraction indicated that when the relative humidity was 55%, the silk films prepared were mainly composed of Silk I structure, whereas silk films formed on other relative humidity had a higher Silk II structure. Fourier transform infrared analysis (FTIR) results also conformed that the secondary structure of silk fibroin can be controlled by changing the humidity of the films formed process. Thermal analysis results revealed Silk I structure was a stable crystal, and the degradation peak increased to 320°C, indicating a greater thermal stability of these films formed under the 55% relative humidity conditions. Atomic force microscopy (AFM) results depicted silk fibroin in the fresh solution had many nanospheres existing with 20–50 nm diameters and mainly maintained a random coil structure without specific nanostructures. At the same time, it also illustrated the self-assembly process of silk fibroin in the aqueous solution without any human intervention. In addition, this present study also provided additional support for self-assembly mechanism of silk fibroin films formation. © 2012 Wiley Periodicals, Inc. J Appl Polym Sci 125: 2148–2154, 2012

Key words: silk fibroin; Silk I; self-assembly; AFM

INTRODUCTION

Silk fibroin (SF) is a typical natural fibroin protein that forms the filaments of silkworm silk and shows unique physical and chemical properties.[1,2] SF has been made into various forms, such as membranes,[3,4] fibers,[5] powders, microspheres,[6] and porous scaffolds,[7,8] depending on its applications. Because of its unique properties such as biocompatibility, biodegradability,[9,10] and high tensile strength,[11] SF is currently being explored for various biomaterial applications. Regenerated silk fibroin solution can be processed into various formations of materials normally stabilized by the induction of β-sheet formation through the use of solvents[12] or by physical stretching.[13] The microstructure of regenerated silk fibroin materials can be changed by chemical modification and so on. However, further investigation is needed to explore a longstanding stability behavior structure and properties of biological materials through green process, such as their unique mechanical properties, and their biodegradation and biocompatibility.

The aqueous solution behavior of silk fibroin is of interest due to the novel self-assembly. Molecular self-assembly, by definition, is the spontaneous organization of molecules under thermodynamic equilibrium conditions into structurally well-defined and rather stable arrangements through a number of noncovalent interactions.[14–17] The aqueous solution behavior and ultimately the material properties of silk fibroin films formed relate to the self-assembly processes. The silk fibroin self-assembly is to design the molecular building blocks that are able to undergo spontaneously stepwise interactions and assemblies through the formation of numerous noncovalent weak chemical bonds such as hydrogen bonds, etc. Although each of the bonds is rather weak, the collective interactions can result in very stable structure and materials.

In the present study, we focused on elucidation of individual and cooperative roles of various environmental factors such as temperature, relative humidity (RH) in controlling the film forming process of silk fibroin self-assembly and influencing the structure and properties of silk fibroin films. At the same time, the goal of the present study was to analysis the role of water in silk fibroin material stabilization processes. In particular, the films forming process was to more closely the natural process during silk processing, concentrated very slowly at the same levels of temperature and humidity to allow sufficient time for the high and low molecular weight fibroin chains (almost 390 KDa and 25 KDa,

Correspondence to: B. Zuo (bqzuo@suda.edu.cn).

respectively) to self-assembly.[18] In addition, physical structure, thermal behavior, and chemical properties of silk fibroin films were examined by means of various analytical techniques.

MATERIALS AND METHODS

Preparation of silk fibroin solutions

Bombyx mori silk fibroins were prepared according to the following procedures. Raw Bombyx mori silk fibers were boiled three times, each time for 30 min in an aqueous solution of 0.5 wt % Na_2CO_3, and then rinsed thoroughly with deionized water to extract sericin proteins. After drying, the degummed silk fibroin was dissolved in a mixture of solvent composed of LiBr/Ethanol/H_2O (45/44/11, wt/wt/wt) at 70°C for 4 h, yielding a 10 g/dL solution. This solution was dialyzed against deionized water using dialysis tubes with a cut off ≈8000–14,000 KDa (Sigma, St. Louis, MO, USA) for 4 days to remove the salt. The solution was optical clear after dialysis and was filtered to remove small amounts of aggregates. And then, the silk fibroin aqueous solution was obtained.

Silk fibroin film formation

To prepare silk fibroin films 60 mL of silk fibroin aqueous solution was cast on glass dishes (diameter 85 mm). The solution was slowly dried to obtain the regenerated silk fibroin films at Binder Temperature & Humidity Chamber (Binder, German). In the films forming process, the temperature and humidity were 10°C, 20°C, 35°C and 35%, 55%, 75%, respectively. In addition, the drying time was related to the silk fibroin solution concentration. So, the final concentration of aqueous silk solution was about 2.0%. Under different environmental conditions, various silk fibroin films were formed and listed in Table I.

TABLE I
Various Silk Fibroin Films Prepared by Different Environmental Conditions

Silk fibroin films sample	Temperature (°C)	Relative humidity (%)
1	10	35
2	10	55
3	10	75
4	20	35
5	20	55
6	20	75
7	35	35
8	35	55
9	35	75

Atomic force microscopy

The morphology of silk fibroin in solution was observed by AFM (Veeco, CA) in air. A 225 μm long silicon cantilever with a spring constant of 3 N/m was used in tapping mode. To clearly characterize the state of silk fibroin in aqueous solution, different concentration of silk fibroin solution was diluted with deionized water.

Scanning electron microscopy

The surface morphologies and cross-sections of silk fibroin films were platinum-coated and examined by scanning electron microscopy (SEM; S4800, Hitachi, Japan). Cross-sections samples were prepared by freezing fracture the dried silk fibroin films in liquid nitrogen.

Fourier transform infrared analysis

The structure of various silk fibroin films was analyzed by Fourier transform infrared analysis (FTIR) on Nicolet5700 (Thermo Nicolet Company) in transmittance mode. For each measurement, each spectrum was obtained by the performance of 32 scans with the wave number ranging from 400 cm^{-1} to 4000 cm^{-1} at intervals of 1 cm^{-1}, with a resolution of 4 cm^{-1}.

Wide angle X-ray diffraction

To investigate the crystalline structure of the silk fibroin films, wide angle X-ray diffraction (WAXD) experiments were measured on X Pert-Pro MPD (PANalytical, Netherlands) in transmittance mode. The incident beam wavelength was 0.154056 nm. The intensity was finally corrected for changes in the incident beam intensity, sample absorption, and background.

Thermogravimetric differential thermal analysis

The thermal stability of silk fibroin films was characterized using Diamond thermogravimetric differential thermal analysis (TG/DTA; Perkin–Elmer Instrument) under a dry nitrogen gas flow of 20 mL/min. The samples were heated from 30°C to 600°C, and the heating rate was 10°C/min.

RESULTS AND DISCUSSION

Structure characteristics

Changes in the structure of the silk fibroin films prepared by different environmental parameters were analyzed by WAXD and FTIR spectroscopy. In previous researches, three silk fibroin conformations have been identified by X-ray diffraction and

infrared spectroscopy: random coil, α-form (Silk I, type II β-turn), and β-form (Silk II, anti-parallel β-pleated sheet).[19,20] The corresponding *d* spacing for Silks I and II are as follows (in nm): 0.98 (II), 0.74 (I), 0.56 (I), 0.48 (II), 0.44 (I), 0.43 (II), 0.41 (I), 0.36 (I), 0.32 (I), and 0.28 (I).[19] However, the 0.74 nm peak occurs in a region of scattering space well removed from peaks found in the Silk II structure.[21] So, the peak at the spacing near 0.75 nm is a strong evidence for Silk I structure.

Figure 1 showed the WAXD data for silk fibroin film samples prepared under different temperature and humidity conditions. Figure 1(A) depicted the silk fibroin films formed at 10°C. In Figure 1(A), samples 1 and 3 exhibited the typical structure, characterized by the presence of a broad peak in the diffraction angle range (for a wavelength of 0.154056 nm) from 5° to 40°. However, sample 2 showed the typical Silk I structure, have 11.9°, 19.6°, 22.2°, 24.5°, 27.7°, 32.4°, 36.8°, corresponding to the Silk I crystalline spacing of 0.75, 0.46, 0.41, 0.37, 0.33, 0.28, 0.26 nm. No typical diffraction peaks of Silk II structure were found in sample 2, which was formed under 10°C and 55% RH environmental condition.

Figure 1(B) depicted the WAXD data for silk fibroin films formed at 20°C. Samples 4 and 6 [Fig. 1(B)] also exhibited the typical crystal structure. That is to say, the structure of silk fibroin films was completely β-form (Silk II, anti-parallel β-pleated sheet). Sample 5 was characterized by diffraction peak at 2θ values of 11.9°, 19.7°, 23.5°, 27.4°, 36.9°, corresponding to the Silk I crystalline *d* spacing of 0.75 (I), 0.46 (I), 0.39 (I), 0.33 (I), 0.26 (I), respectively. At the same time, sample 8 [Fig. 1(C)] also showed the Silk I crystal structure, having five obviously diffraction peaks at 11.9°, 19.8°, 24.2°, 27.6°, 36.8°, corresponding to the crystalline *d* spacing of 0.75 (I), 0.46 (I), 0.38 (I), 0.33 (I), 0.26 (I), respectively. In addition, sample 9 [Fig. 1(C)] contained small amounts of Silk I structure, having the diffraction peaks at 11.9° and 19.8°. Moreover, sample 7 showed the typical Silk II structure.

Seen from the above analysis that samples 2, 5, and 8 formed under the 55% RH conditions exhibit obviously the Silk I crystal structure, not Silk II structure. This result indicates that the environmental humidity has a significant influence on the formation of Silk I structure. That is to say, relative humidity adjusts the drying rate of the silk fibroin aqueous solution and controls the self-assembly process of silk fibroin. So, water has notable effect on the formation of Silk I structure.

Structure changes in the silk fibroin films after different environmental conditions formed were characterized by FTIR (Fig. 2). The infrared spectral region within 1700 cm^{-1}–1500 cm^{-1} is assigned to the absorption bands by the amide I (1700 cm^{-1}–1600 cm^{-1}) and amide II (1600 cm^{-1}–1500 cm^{-1}), which have been

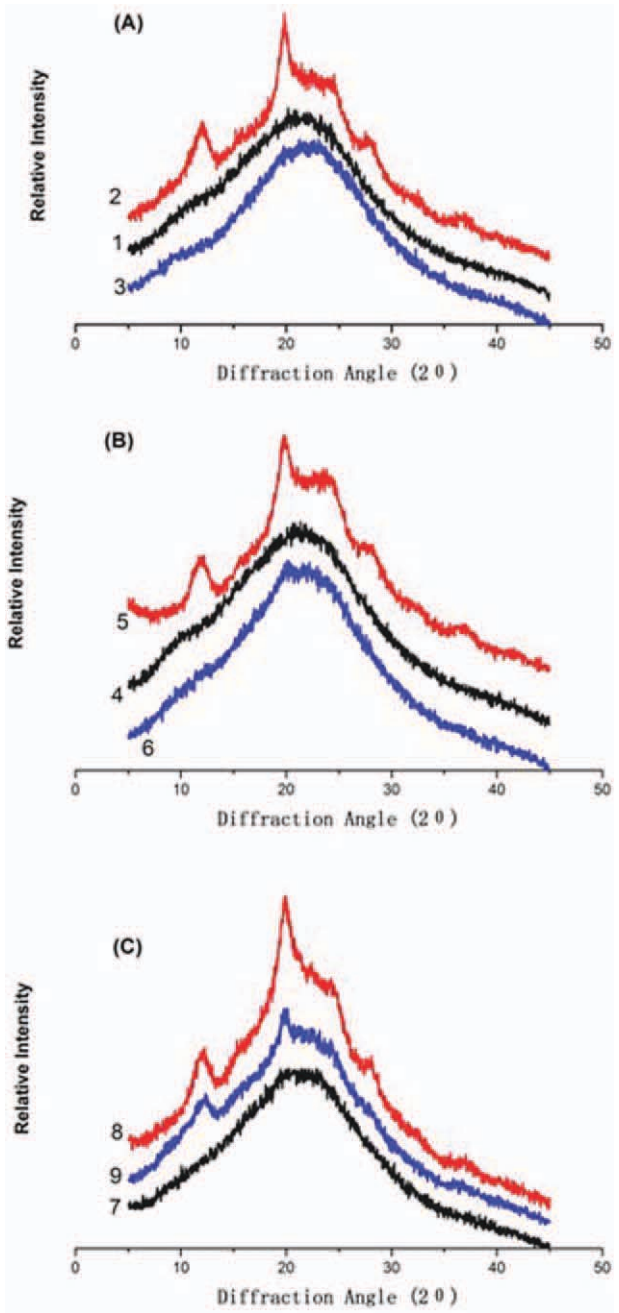

Figure 1 WAXD data for silk fibroin films prepared at different conditions. A, B, and C at 10°C, 20°C, and 35°C, respectively. [Color figure can be viewed in the online issue, which is available at wileyonlinelibrary.com.]

used for the analysis of different secondary structures of silk fibroin. The peaks at 1610 cm^{-1}–1630 cm^{-1} (amide I) and 1510 cm^{-1}–1520 cm^{-1} (amide II) are characteristic of Silk II structure.[19] At the same time, the peaks at 1648 cm^{-1}–1554 cm^{-1} (amide I) and 1535 cm^{-1}–1542 cm^{-1} are attributed to random coil, other studies have revealed that these peaks correspond to the Silk I conformation.[22] In the present study, the sample 1 showed one strong peak at 1625 cm^{-1}, corresponding to Silk II β-sheet. At the same time, one

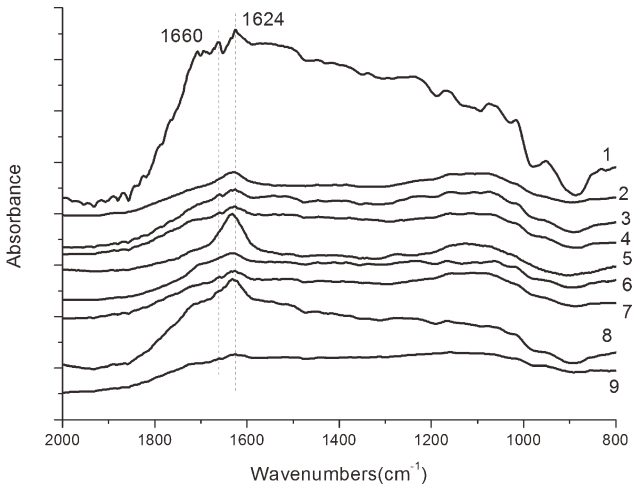

Figure 2 FTIR spectra of silk fibroin films prepared by different environmental conditions.

shoulder peak appeared at 1648 cm^{-1}, corresponding to random coil structure. Samples from 2 to 9 showed one peak at 1625 cm^{-1}–1631 cm^{-1}. The same trend in structure change was also found in the amide II region. So, the FTIR results are consistent with the WAXD results, confirming that the secondary structure of silk fibroin can be controlled by changing the humidity of the film formed process.

In this present research, Silk I crystal structure is directly formed when the relative humidity was 55%. This film process is very slow to allow sufficient time for silk fibroin molecular chain self-assembly. More importantly, the formation of Silk I crystal structure is mainly related to the humidity, while the temperature is not obvious. The results reveal that it is an inherent ability of the silk fibroin to self-assembly into Silk I structure by controlling the environmental humidity, although other factors such as pH, salts, and solution concentration can affect the self-assembly process.[15]

Thermal analysis

Figure 3 depicts standard DTA curves for the silk fibroin films prepared by different environmental conditions. The silk fibroin films samples 1, 4, and 7 formed under 35% RH conditions. In Figure 3(A), the silk fibroin film samples 1, 4, and 7 showed an endothermic peak at around 100°C, a crystallization peak at 244°C–262°C, a degradation peak at about 300°C, and an exothermic peak at 310°C. The endothermic peak at around 100°C was due to the evaporation of bound water and indicated that these samples interacted with water. At the crystallization peak random coil and α-helix structures were transformed to β-sheet. After the appearance of the crystallization peak, the degradation of the silk fibroin films occurred at around 300°C.

The silk fibroin film samples 2, 5, and 8 were formed under the 55% RH of environmental conditions [Fig. 3(B)]. The sample 2 exhibited an endothermic peak at around 124°C, a small crystallization peak at 259°C, and a degradation peak at 317°C, with a small shoulder peak at 324°C. However, samples 5 and 8 depicted the endothermic peak at 123°C

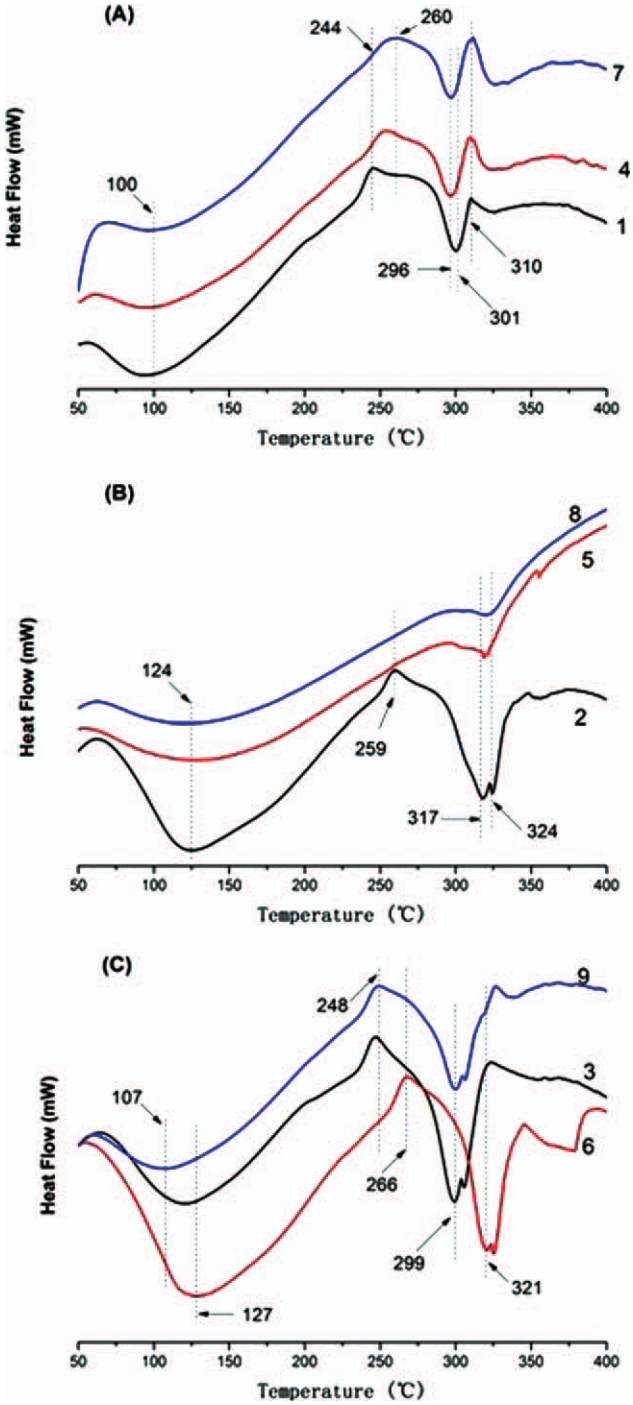

Figure 3 DTA curves for silk fibroin films prepared at different conditions; Figure 3A, B, and C at 10°C, 20°C, 35°C, respectively. [Color figure can be viewed in the online issue, which is available at wileyonlinelibrary.com.]

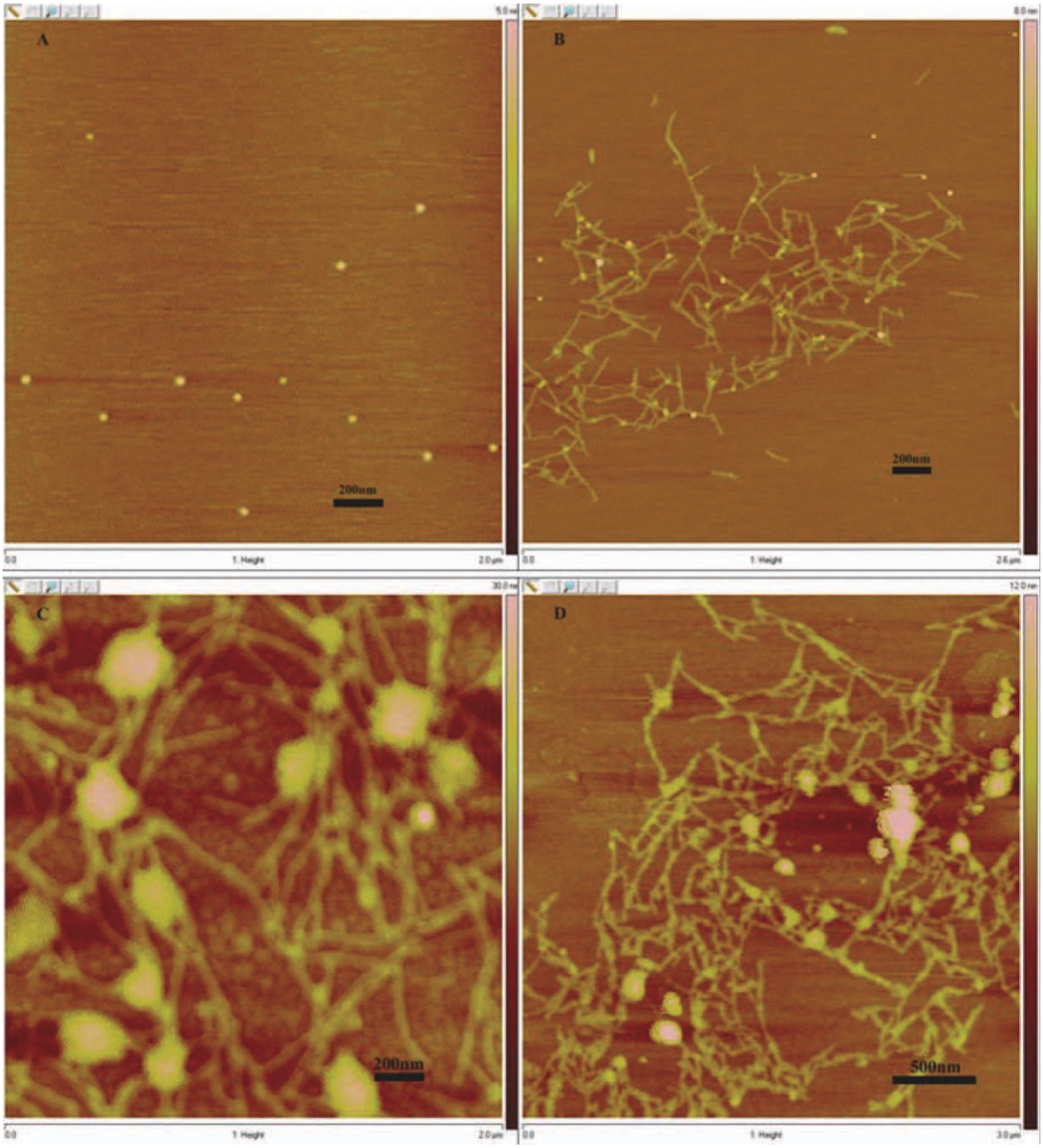

Figure 4 AFM images obtained by various concentrations of silk fibroin solution. A: 1.88%; B: 2.16%; C: 4.07%; D: 5.70%. [Color figure can be viewed in the online issue, which is available at wileyonlinelibrary.com.]

disappeared. This phenomenon implied that the silk fibroin films became hydrophobic. At the same time, the crystallization peak also disappeared, implying that Silk I is a stable crystal, never transforming to β-sheet structure.[19] According to the WAXD and FTIR results confirmed that the silk fibroin film 2, 5, and 8 samples were composed of Silk I crystal structure, not Silk II structure. In addition, the degradation peak increased to 320°C, indicating a greater thermal stability of these films.

However, when the relative humidity was 75%, the silk fibroin film samples 3, 6, and 9 were formed [Fig. 3(C)]. These three samples illustrated an endothermic peak at around 107–127°C. This endothermic peak was due to the evaporation of bound water and demonstrated that the silk fibroin films interacted with water. The sample 6 showed a crystallization peak at 266°C higher than the samples 3 and 9, at the same time, the degradation peak of sample 6 at 321°C also were higher than samples 3 and 9. This result implied that higher unstable non-crystal structure was transformed to β-sheet in the sample 6. The degradation temperature should be related to influence the thermal stability of silk fibroin film. It

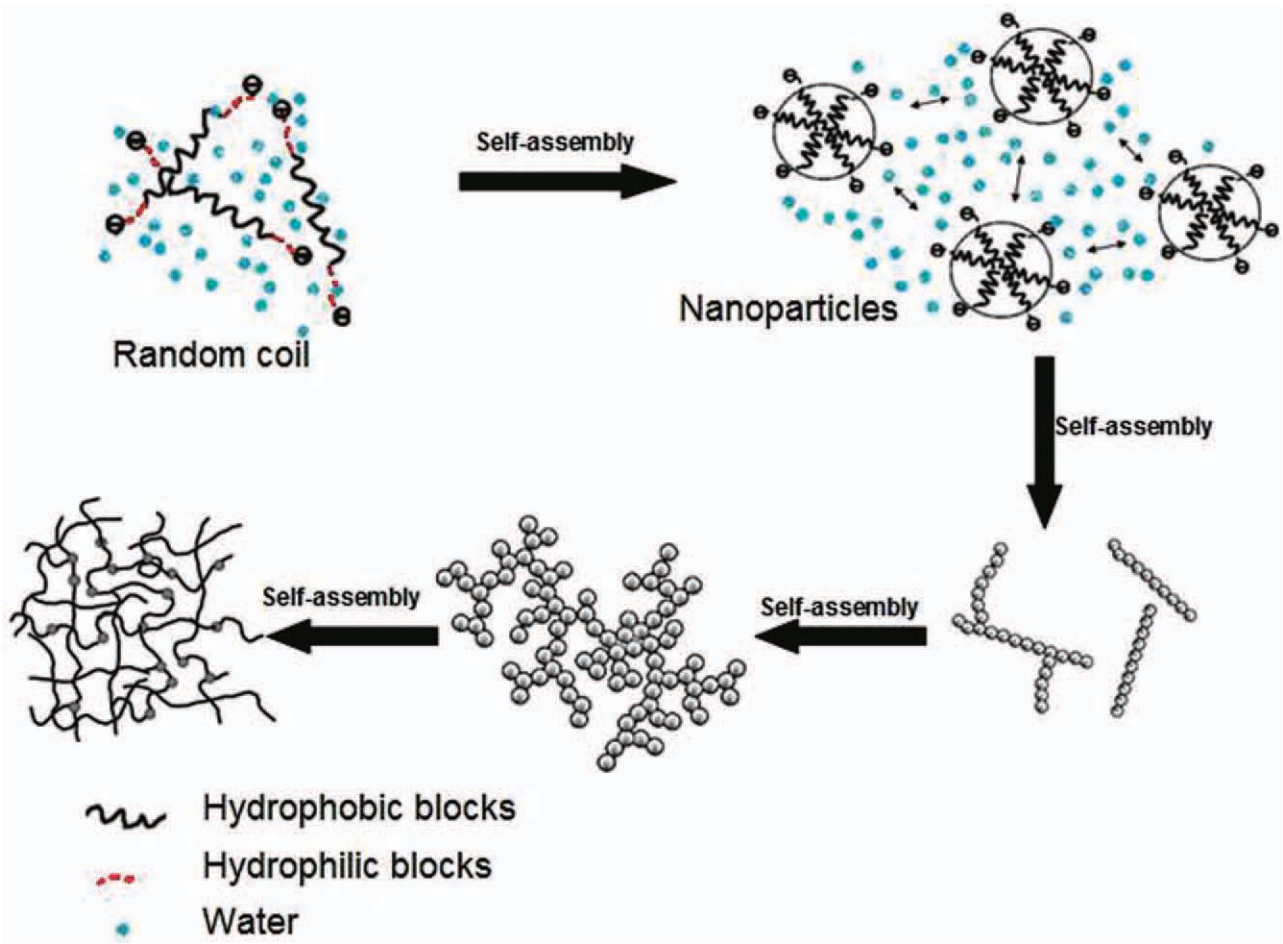

Figure 5 Schematic of the self-assembly mechanism of silk fibroin in aqueous solution. [Color figure can be viewed in the online issue, which is available at wileyonlinelibrary.com.]

is important that the thermal stability is concerned with the β-sheet contents.

Morphology

In the present study, to investigate the self-assembly process in the silk fibroin aqueous solution, various concentrations of silk fibroin solution were characterized by AFM providing more details and precise information on the morphology of the silk fibroin aqueous solution (Fig. 4). Figure 4(A) depicted the nanospheres existing with 20–50 nm diameters in the fresh silk fibroin aqueous solution in which the concentration was about 1.88%. With the concentration increasing, nanowires were composed with many nanospheres by self-assembly [Fig. 4(B)]. These nanowires had the length more than 100 nm, with the diameter of about 20 nm. At the same time, some nanospheres existed in the solution with 40 nm diameter. In the self-assembly process, the challenge in molecular self-assembly was to design molecular building blocks that could undergo spontaneous organization into a well-defined and stable macroscopic structure using non-covalent bonds. These bonds included hydrogen bonds, ionic bonds, water-mediated hydrogen bonds, hydrophobic and van der Waals interactions, etc.[23] Although each force was rather weak, nanowires slowly formed the network structure by means of these forces without any intervention in the silk fibroin aqueous solution [Fig. 4(B)]. With further increase of concentration, nanowires morphology in the silk fibroin aqueous solution was again evidenced [Fig. 4(C,D)].

Figure 4 illustrated the nanostructure of silk fibroin in fresh solution. Interestingly, silk fibroin in the fresh solution mainly maintained a random coil structure without specific nanostructures. This result was also evidenced by Lu et al.[24,25] In the silk fibroin aqueous solution, self-assembly was a spontaneous process without any human intervention. A schematic representation of silk fibroin self-assembly process is shown in Figure 5. When silk fibroin maintained a random coil structure, extensive time and energy were required to rearrange the hydrophobic and hydrophilic blocks of the protein chains in the silk fibroin chains. Once the hydrophobic and

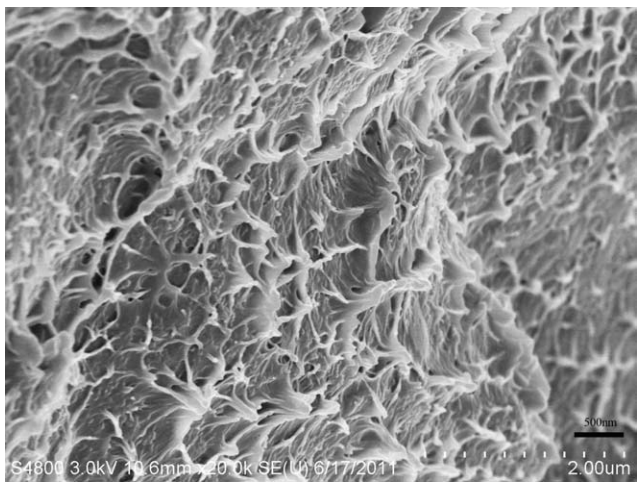

Figure 6 SEM images of cross-section of silk fibroin films obtained by lyophilization.

hydrophilic blocks of the protein chains had rearranged and assembled into nanoparticles, self-assembly process was confirmed (Fig. 4). With the releasing of water, the hydrophobic and hydrophilic blocks further assembled to form more nanospheres, and then connected to the irregular network. Finally, the silk fibroin films formed might be stabilized by its strong inter- and intra-molecular interactions from the removal of the water. Figure 6 confirmed the nanofilaments existed in the silk fibroin films.

Under different environmental conditions, self-assembly is a spontaneous process without any human intervention, but it can affect the transition from random coil structure to crystal structure, even finally impacts the properties of silk fibroin films. This must continue to further research in this field. At the same time, the present study also provides additional support for self-assembly mechanism of silk fibroin films formation.

CONCLUSIONS

By controlling the environmental temperature and relative humidity, the Silk I structure of the films can be prepared directly from silk fibroin aqueous solution under the 55% relative humidity. WAXD and FTIR results confirmed Silk I structure existing in the films formed, when the relative humidity was 55%. Thermal analysis showed that the crystallization peak of this film disappeared, implying that Silk I structure is a stable crystal structure, never transforming to β-sheet structure. At the same time, the degradation peak increased to 320°C, indicating Silk I crystal structure is a reasonably stable structure in terms of material and function. AFM results illustrated silk fibroin in the fresh solution had many nanospheres existing with 20–50 nm diameters and mainly maintained a random coil structure without specific nanostructures. At the same time, it also showed the self-assembly process of silk fibroin macromolecular in the aqueous solution without any human intervention. Different environmental temperature and relative humidity can control the drying rate of the silk fibroin aqueous solution. It will influence the self-assembly process of silk fibroin. In addition, this research may provide some support for the self-assembly mechanism of silk fibroin in aqueous solution, and this silk films have potential applicability for a variety of biodegradable materials due to its specific Silk I structure.

The authors acknowledge support from the First Phase of Jiangsu Universities' Distinctive Discipline Development Program for Textile Science and Engineering of Soochow University, National Engineering Laboratory for Modern Silk Project, and Suzhou Science and Technology Plan Project (SG201046).

References

1. Wenk, E.; Wandrey, A. J.; Merkle, H. P.; Meinel, L. J Control Release 2008, 132, 26.
2. Park, W. H.; Jeong, L.; Yoo, D.; Hudson, S. Polymer 2004, 45, 7151.
3. Lawrence, B. D.; Omenetto, F.; Chui, K.; Kaplan, D. L. J Mater Sci 2008, 43, 6967.
4. Bray, L. J.; George, K. A.; Ainscough, S. L.; Hutmacher, D. W.; Chirila, T. V.; Harkin, D. G. Biomaterials 2011, 32, 5086.
5. Amiraliyan, N.; Nouri, M.; Kish, M. H. Polym Sci A 2010, 52, 407.
6. Cao, Z.; Chen, X.; Yao, J.; Huang, L.; Shao, Z. Soft Matter 2007, 3, 910.
7. Mandal, B. B.; Kundu, S. C. Biomaterials 2009, 30, 2956.
8. Nazarov, R.; Jin, H. J.; Kaplan, D. L. Biomacromolecules 2004, 5, 718.
9. Horan, R. L.; Antle, K.; Collette, A. L.; Wang, Y.; Huang, J.; Moreau, J. E.; Volloch, V.; Kaplan, D. L.; Altman, G. H. Biomaterials 2005, 26, 3385.
10. Lammel, A. S.; Hu, X.; Park, S. H.; Kaplan, D. L.; Scheibel, T. R. Biomaterials 2010, 31, 4583.
11. She, Z.; Zhang, B.; Jin, C.; Feng, Q.; Xu, Y. Polym Degrad Stab 2008, 93, 1316.
12. Tsukada, M.; Gotoh, Y.; Nagura, M.; Minoura, N.; Kasai, N.; Freddi, G. J Polym Sci Part B Polym Phys 1994, 32, 961.
13. Jin, H. J.; Park, J.; Karageorgiou, V.; Kim, U. J.; Valluzzi, R.; Cebe, P.; Kaplan, D. L. Adv Funct Mater 2005, 15, 1241.
14. Zhang, S. Biotechnol Adv 2002, 20, 321.
15. Lehn, J. M. Supramolecular Chemistry: Concepts and Perspectives; VCH: Weinheim, 1995.
16. Whitesides, G. M.; Simanek, E. E.; Mathias, J. P.; Seto, C. T.; Chin, D.; Mammen, M.; Gordon, D. M. Acc Chem Res 1995, 28, 37.
17. Philp, D.; Stoddart, J. F. Angew Chem Int Ed Engl 1996, 35, 1154.
18. Matsumoto, A.; Lindsay, A.; Abedian, B.; Kaplan, D. L. Macromol Biosci 2008, 8, 1006.
19. Lu, Q.; Hu, X.; Wang, X.; Kluge, J. A.; Lu, S.; Cebe, P.; Kaplan, D. L. Acta Biomater 2010, 6, 1380.
20. Rusa, C. C.; Bridges, C.; Ha, S. W.; Tonelli, A. E. Macromolecules 2005, 38, 5640.
21. Philip, A. J. Biopolymer 1998, 45, 307.
22. Wilson, D.; Valluzzi, R.; Kaplan, D. L. Biophys J 2000, 78, 2690.
23. Zhang, S.; Marini, D. M.; Hwang, W.; Santoso, S. Curr Opin Chem Biol 2002, 6, 865.
24. Lu, Q.; Huang, Y.; Li, M.; Zuo, B.; Lu, S.; Wang, J.; Zhu, H.; Kaplan, D. L. Acta Biomater 2011, 7, 2394.
25. Wang, X.; Kim, H. J.; Xu, P.; Matsumoto, A.; Kaplan, D. L. Langmuir 2005, 21, 11335.